

# Probabilistic Analysis of Time-Dependent Failure of SiC/SiC Composite Claddings

Chen Hu<sup>1</sup>, Joseph F. Labuz<sup>2</sup>, Takaaki Koyanagi<sup>3</sup>, and Jia-Liang Le<sup>4</sup>

**Abstract:**

## 1. Introduction

The 2011 Fukushima Daiichi nuclear power plant accident has stimulated the active development of accident-tolerant fuels (ATFs) and accident-tolerant cores. In recent years, silicon carbide (SiC) fiber-reinforced SiC matrix (SiC/SiC) composites have attracted increasing attention as an alternative material for fuel cladding in light water reactors (LWRs) [11]. Extensive experimental research showed that the SiC/SiC composites can retain excellent mechanical properties under high temperature and neutron irradiation conditions. Compared to traditional Zirconium alloy cladding and core, which would produce explosive hydrogen in a water vapor environment, SiC/SiC composites exhibit general chemical inertness at very high temperature [25]. Moreover, they are also stable under irradiation. Owing to these attractive features, SiC/SiC composites are considered favorably as a promising material that provides passive safety for LWRs in beyond-design-basis severe accident scenarios [29].

For LWR claddings, SiC/SiC composites are fabricated in the form of long tubes. A number of investigations were performed on mechanical the behaviors of SiC/SiC composite tubes under different loading scenarios including uniaxial tension, internal pressure, and multiaxial loading [19, 5, 6, 21]. It was observed that, under uniaxial loading, the specimen first exhibits a linear elastic behavior up to a stress level, which is referred to as the proportional limit stress (PLS). Beyond this stress, the matrix material experiences damage, which is manifested by a degradation of elastic stiffness. The progression of matrix damage eventually leads to localized fiber break, and the specimen attains its ultimate tensile strength (UTS). Upon further displacement-controlled loading, the specimen would exhibit a softening behavior. For the purpose of cladding design, the PLS and UTS are two critical metrics. The PLS indicates the stress level at damage initiation, which poses risk of loss of fission gas retention, whereas at UTS the structure experiences extensive damage, which deteriorates its load capacity. An inter-laboratory round robin study was recently performed to measure axial tensile properties of same batch of SiC/SiC composites tubular specimens. 43 specimens were tested and it was reported that the coefficients of variation of PLS and UTS are 9.7% and 12.5%, respectively [22].

The randomness of strength of SiC/SiC composites can be attributed to the heterogeneity of the material. **In the manufacturing process, the SiC matrix is deposited from gaseous reactants on to a heated substrate of fibrous preforms (SiC) [13]. This process, called Chemical Vapour Infiltration (CVI), inevitably introduces internal pores in the matrix.** It was reported that the porosity of CVI SiC/SiC composites is in the range of 8-17% [12, 5]. By using computed X-ray tomography, it has observed that the large pores between fiber tows are crucial to damage development compared to small pores [20]. The size and location of these internal pores are inherently random causing randomness in both local stress field and material resistance and consequently the macroscopically observed variability in PLS and UTS.

The randomness of PLS and UTS has important implications for design of SiC/SiC composite claddings. It is widely acknowledged that engineering structures must be designed against an acceptable risk level. In the current design approach, an empirical reduction factor is applied to the

---

<sup>1</sup>Department of Civil, Environmental, and Geo- Engineering, University of Minnesota.

<sup>2</sup>Department of Civil, Environmental, and Geo- Engineering, University of Minnesota.

<sup>3</sup>Materials Science and Technology Division, Oak Ridge National Laboratory.

<sup>4</sup>Department of Civil, Environmental, and Geo- Engineering, University of Minnesota, Minneapolis, Minnesota. Corresponding author.

PLS to account for its uncertainty [17]. This concept is similar to the safety factors used in design of concrete and steel structures. The safety factors allow us to perform reliability-based structural design through deterministic analysis. The essential step is to relate the safety factors to the failure risk of the structure [8, 14, 2]. Evidently this relation must be derived from a probabilistic model of structural failure.

In recent years, considerable attention has been directed towards investigation of the failure statistics of SiC/SiC composites. Previous studies have largely used the two-parameter Weibull distribution for the probability distributions of PLS and UTS [22, 24, 7]. The Weibull distribution belongs to the class of extreme value statistics [27, 28, 26, 2], which indicates that the failure statistics of the structure can be represented by an infinite weakest-link model. Physically it implies a damage localization mechanism and furthermore that the structure is much larger than the size of the damage zone. A series of recent studies discussed the applicability of the Weibull distribution for strength statistics of structures made of quasibrittle materials, such as composites and ceramics, which feature a strain softening behavior and damage localization mechanism [3, 1, 16, 2]. It was shown that, for most quasibrittle structures, the structure size is not sufficiently large to guarantee the validity of the Weibull distribution. The same issue also applies to SiC/SiC composite tubes. The laboratory test specimen is less than 100 mm long, which is not significantly larger than the size of the damage zone. Therefore, the classical Weibull model cannot be used to extrapolate the laboratory test result to full-scale cladding design.

In addition to the inapplicability of the Weibull distribution for design extrapolation, probabilistic modeling of SiC/SiC composite tubes is further complicated by the time evolution of applied loading. A thermomechanical analysis was recently performed to investigate the loading history of the SiC/SiC cladding over its service lifetime [4, 23]. It was shown that the cladding experiences complicated time-dependent loading along axial and hoop directions in LWRs. To model the lifetime of the cladding, it is crucial to take into account of the damage accumulation mechanism. The failure probability of the entire structure at the present time is not only dependent on current stress state but also on the prior loading history. So far, such a time-dependent model has not been investigated.

In this study, we develop a time-dependent probabilistic model for lifetime of SiC/SiC cladding. The model is anchored by integration of a finite weakest-link statistical model and a time-dependent damage accumulation model. The paper is planned as follows: Section 2 discusses the time-dependent failure model; Section 3 describes the finite weakest-link model; Section 4 applies the model to reliability analysis of SiC/SiC cladding, and Section 5 discusses the result of the analysis and its implications.

## 2. Probabilistic Time-Dependent Failure Model

Over the past years, extensive efforts were devoted toward laboratory testing of SiC/SiC tube specimens, and major advances have been made [19, 5, 6, 21]. The development of experimental techniques led to an improved understanding of the failure behavior of laboratory test specimens. The laboratory specimens usually have the same cross-sectional dimension as the fuel cladding, but the specimen length is about two orders of magnitude shorter than the cladding. The essential question is how to predict the failure statistics of the full-size cladding from the laboratory test results. For such a prediction, we first need a robust probabilistic model for the failure of the test specimen.

Consider a laboratory test specimen under general loading (axial load  $F$ , internal pressure  $p$ , and torsion  $T$ ). The structural design is largely concerned with the load carrying capacity, which can be described by the strength-based failure criterion. To formulate such a criterion, we first define the

following nominal stresses:

$$\sigma_{\theta\theta} = \frac{r_i^2(r_m^2 + r_e^2)}{r_m^2(r_e^2 - r_i^2)}p \quad (1)$$

$$\sigma_{zz} = \frac{F + p\pi r_i^2}{\pi(r_e^2 - r_i^2)} \quad (2)$$

$$\sigma_{z\theta} = \frac{3T}{2\pi(r_e^3 - r_i^3)} \quad (3)$$

where  $r_i$ ,  $r_e$  are the inner and outer radius of the specimen, respectively, and  $r_m = 0.5(r_i + r_e)$ . While these nominal stresses can be considered as load parameters in the dimension of stress, they physically represent the homogenous elastic stresses of the test specimen.

Here we consider that the specimen will fail under control loads once the following criterion is met [5]:

$$F(\sigma_i, k_i) = k_1\langle\sigma_1\rangle^2 + k_1\langle\sigma_2\rangle^2 + k_2\langle\sigma_1\rangle\langle\sigma_2\rangle + k_3\sigma_3^2 - 1 \geq 0 \quad (4)$$

where  $\sigma_1, \sigma_2 =$  in-plane principal elastic stresses,  $\sigma_3 = \sigma_{\theta\theta} - \sigma_{zz}$ ,  $k_i$  ( $i = 1, 2, 3$ ) = model constants, and  $\langle x \rangle =$  Macaulay bracket =  $\max(x, 0)$ . By considering some specific loading scenarios, such as uniaxial tension, uniaxial compression, and equi-biaxial tension, we can express  $k_i$ 's by

$$k_1 = \frac{1}{f_t^2} - \frac{1}{f_c^2}; \quad k_2 = \frac{1}{f_b^2} - 2k_1; \quad k_3 = \frac{1}{f_c^2} \quad (5)$$

where  $f_t$ ,  $f_c$  and  $f_b$  denote the nominal strengths of the specimen corresponding to the uniaxial tensile, uniaxial compressive, and biaxial tensile stress states, respectively. It is worthwhile to note that the nominal strengths are structural properties, which could vary with the specimen length. Therefore, the failure criterion itself (Eq. 4) is dependent on the specimen length.

By considering the nominal strengths as random variables, the failure probability of the test specimen under given loading can be expressed by

$$P_f(\sigma_i) = 1 - \Pr[F(\sigma_i, f_t, f_c, f_b) \leq 0] \quad (6)$$

$$= 1 - \iiint_{\Omega} f(x, y, z) dx dy dz \quad (7)$$

where  $x, y, z$  denote the random values of  $f_t, f_c$ , and  $f_b$ , respectively,  $\Omega$  denotes the region of  $F(\sigma_i, x, y, z) \leq 0$ , and  $f(x, y, z)$  is the joint probability density function (pdf) of random variables  $f_t, f_c$ , and  $f_b$ .

The foregoing analysis is anchored by a strength-based failure criterion. In actual applications, the SiC/SiC claddings are subjected to time-dependent loading, which is lower than the structural strength. The key design parameter is the structural lifetime. Therefore, it is necessary to reformulate the failure criterion (Eq. 4) for calculating the lifetime. To this end, we consider a damage kinetics model, through which the nominal strengths can be related to the specimen lifetime. Following the framework of continuum damage mechanics [18, 9, 10], we introduce a damage parameter  $\omega$ , which ranges from 0 (intact) to 1 (fully damaged).

$$\frac{d\omega}{dt} = \frac{\phi(\omega)}{[k - g(\sigma_i)]^n} \quad (8)$$

where  $g(\sigma_i) = k_1\langle\sigma_1\rangle^2 + k_1\langle\sigma_2\rangle^2 + k_2\langle\sigma_1\rangle\langle\sigma_2\rangle + k_3\sigma_3^2$ , and  $k, n$  are constants.

Note that constants  $k_i$ 's are related to the uniaxial tensile, compressive, and equi-biaxial tensile strengths. The damage kinetics model implies that the monotonic nominal strengths would depend on the loading rate. Let  $r_t, r_c$ , and  $r_b$  denote the loading rates used in the uniaxial tensile, compressive,

and equi-biaxial tensile experiments, respectively. These experiments directly measure the nominal strengths and consequently constants  $k_i$ 's.

To relate the monotonic nominal strengths to the specimen lifetime, we now consider two loading protocols: 1) reference linearly ramped loading and 2) general time-dependent loading. For the reference linearly ramped loading, we consider  $\sigma_i = r_i t$ , where  $r_1 = r_t + r_b$ ,  $r_2 = r_b$ , and  $r_3 = r_t + r_c$ . These reference loading rates are determined by superimposing the loading rates used in the relevant strength tests. By applying the separation of variables to Eq. 8, we can express the relation between the damage extent and the by

$$\int_0^{\omega_c} \frac{d\omega}{\phi(\omega)} = \int_0^{t_c} \frac{dt}{(k - \alpha t^2)^n} \quad (9)$$

where  $\alpha = k_1 \langle r_1 \rangle^2 + k_1 \langle r_2 \rangle^2 + k_2 \langle r_1 \rangle \langle r_2 \rangle + k_3 r_3^2$ ,  $\omega_c =$  critical damage extent at which the specimen fails under load controlled test, and  $t_c =$  time at failure. Meanwhile, the strength-based failure criterion (Eq. 4) indicates  $\alpha t_c^2 = 1$ , which yields  $t_c = \alpha^{-1/2}$ . By substituting the expression of  $t_c$  into Eq. 9, we obtain

$$\int_0^{\omega_c} \frac{d\omega}{\phi(\omega)} = C/\sqrt{\alpha} \quad (10)$$

where  $C = \int_0^1 (k - x^2)^{-n} dx$ .

Now we consider a general loading history, for which the stress components are expressed by  $\sigma_1(t) = f_t \psi_1(t)$ ,  $\sigma_2(t) = f_t \psi_2(t)$ , and  $\sigma_3(t) = f_t \psi_3(t)$  "here we need to define  $f_t$ , which distinguish from previous  $f_t$ , maybe we can just use  $\psi(t)$ ". Meanwhile, applying the same analysis of the kinetics model to this general loading case yields

$$\int_0^{\omega_c} \frac{d\omega}{\phi(\omega)} = \int_0^{t_f} \frac{dt}{\{k - [k_1 \langle \psi_1(t) \rangle^2 + k_1 \langle \psi_2(t) \rangle^2 + k_2 \langle \psi_1(t) \rangle \langle \psi_2(t) \rangle + k_3 \psi_3^2(t)] f_t^2\}^n} \quad (11)$$

where  $t_f =$  failure time, or the specimen lifetime.

Since the damage growth law (Eq. 8) is formulated for multi-axial loading scenarios, we postulate that for any arbitrary loading the specimen would fail at the same critical damage extent. By equating Eqs. 9 and 11, we obtain

$$\int_0^{t_f} \frac{dt}{\{k - [k_1 \langle \psi_1(t) \rangle^2 + k_1 \langle \psi_2(t) \rangle^2 + k_2 \langle \psi_1(t) \rangle \langle \psi_2(t) \rangle + k_3 \psi_3^2(t)] f_t^2\}^n} = C/\sqrt{\alpha} \quad (12)$$

from which we can solve  $t_f$ . By considering  $f_t$ ,  $f_b$  and  $f_c$  as random variables, we can perform Monte Carlo simulation to determine the probability distribution of  $t_f$  (i.e. lifetime distribution) of the laboratory specimen for a given loading history. This probability distribution exactly equals to the failure probability  $P_{fs}$  of the specimen at any given time  $t$ , i.e.  $\Pr(t_f \leq t) = P_{fs}(t)$ .

### 3. Finite Weakest-Link Model for Design Extrapolation

The foregoing analysis focuses on the failure of laboratory specimens, which are far shorter than the actual LWR claddings. To extrapolate the lifetime distribution of laboratory specimens to the LWR cladding, we need to rely on a statistical model that is consistent with the failure mechanism. In this study, we adopt the finite weakest-link model, which indicates that the specimen survives only if all the material elements survive. This physically represents the damage localization mechanism, which is a salient feature of the failure of quasibrittle materials, a class of materials which the SiC/SiC composites belongs to.

We first apply the finite weakest-link model to the laboratory specimens. We consider that, at failure, damage would localize into one material element. The size of this material element is related to the width of the fracture process zone. For SiC/SiC composites, the size of the material element which damage localizes is expected to be on the order of the tow width ( $\approx 1.2$  mm). By assuming

that the failure statistics of each material element is statistically independent, the failure probability  $P_{fs}(t)$  of the specimen subjected to a general loading history can be calculated by

$$P_{fs}(t) = \Pr(t_f \leq t) = 1 - [1 - P_1(t)]^{n_s} \quad (13)$$

where  $P_1(t)$  = failure probability of one material element, and  $n_s$  = number of material elements in the specimen. Eq. 13 is written by assuming that the all the material elements experience the same stress field. Based on Eq. 13, we can write  $P_1(t)$  as

$$P_1(t) = 1 - [1 - P_{fs}(t)]^{1/n_s} \quad (14)$$

Now we consider an actual SiC/SiC cladding. Recent studies have shown that during its service lifetime the cladding experiences a non-uniform stress distribution. To account for the non-uniformity of the stress field, we can write the finite weakest-link model as

$$P_f(t) = 1 - \prod_{j=1}^n [1 - P_1(\boldsymbol{\sigma}_j, t)] \quad (15)$$

where  $n$  = number of material elements in the cladding, and  $\boldsymbol{\sigma}_j$  = a vector containing the stress components  $\sigma_i$  for  $j$ th material element. Eq. 15 can be conveniently rewritten by taking the logarithmic, which will allow us to replace the product by a summation. Since there are many elements in the cladding, we can write the summation by integration, which gives

$$P_f(t) = 1 - \exp \left\{ \frac{1}{V_0} \int_V \ln \{1 - P_1[\boldsymbol{\sigma}(x, t), t]\} dV \right\} \quad (16)$$

where  $V_0$  = volume of one material element. By substituting Eq. 14 into Eq. 16, we have

$$P_f(t) = 1 - \exp \left\{ \frac{1}{V_s} \int_V \ln \{1 - P_{fs}[\boldsymbol{\sigma}(x, t), t]\} dV \right\} \quad (17)$$

where  $V_s$  = volume of laboratory test specimen.  $P_{fs}[\boldsymbol{\sigma}(x, t), t]$  represents the failure probability of the test specimen at time  $t$  when subjected to stress history  $\boldsymbol{\sigma}(t)$  that is experienced by material point located at  $x$ . As mentioned in Sec. 2,  $P_{fs}[\boldsymbol{\sigma}(x, t), t]$  can be calculated through Monte Carlo simulations based on the known cdf's of  $f_t$ ,  $f_b$  and  $f_c$  through Eq. 12.

Eq. 17 provides a closed-form relationship between the failure statistics of test specimen and the full-size cladding. The model captures both the effects of size and the time-varying load history on the failure probability of the SiC/SiC claddings. As indicated by Eq. 17, for a given load history, an increase in specimen size would lead to an increase in failure probability. This is the key prediction of the present model, which has important consequence for extrapolation of laboratory test results to full-size design. Meanwhile, the use of  $P_{fs}[\boldsymbol{\sigma}(x, t), t]$  indicates that the failure probability at any given time depends on not only the current stress state, but also the previous load history. This dependence arises from the damage kinetics model, which naturally captures the effect of load path on the damage accumulation. The size effect and effect of damage kinetics model on the failure probability will be demonstrated numerically in the subsequent section.

#### 4. Reliability Analysis of SiC/SiC Claddings

In order to demonstrate the effectiveness of our model, one of current thermo-mechanical analysis [23] was selected. Stress evolution profile from that analysis was introduced to our probabilistic time-dependent model and finite weakest-link model. Thus a reliability analysis was performed on SiC/SiC cladding simulated under normal operation conditions. Figure 1 showed an overview of our analysis procedure.

In the foregoing thermo-mechanical analysis, stress history of a 4m length SiC/SiC composites cladding under the service time of 2 years was simulated by Abaqus, which took into account the effect of external pressure, internal pressure, temperature and irradiation induced swelling [23]. The SiC/SiC cladding would experience compression in both axial and hoop direction at the beginning due to initial external pressure and gradually gain towards tension majorly due to the increase of internal pressure. Figure 2 showed variation of axial and hoop stress with time at axial mid-plane of the cladding inner surface. It can be seen that the rate of increase of hoop stress was bigger than that for the axial stress. This can be explained simply by the relation of stresses with the internal pressure for thin-walled cylindrical structure, which is the rate of increase of hoop stress is twice of that for the axial stress.

At the end of 24 months, the maximum tension would occur at the inner surface of the cladding, with 51 MPa tensile stress in axial direction and 73 MPa tensile stress in hoop direction [23]. Figure 3 showed variation of axial and hoop stresses at the inner surface along the height of the cladding during the end of 24 months. It can be seen that for most of the range in height, cladding would experience stress close to maximum tensile stress. The kink close to the end of the cladding was due to irradiation induced swelling under lower temperate. With those stress tensor input, we calculated in-plane principle stresses and eliminate all the compression at early time stage to satisfy the requirements of failure criterion is Eq. 4.

Now for each simulation element in Abaqus, we input the calculated stress data into our model, as well as the strength parameters sampled from Monte Carlo Simulation. During each sampling process, once the failure time  $t_f$  was calculated based on Eq. 12, it would be appended into an array of failure time. The array would be sorted after all the simulation for this element was finished. The failure probability of laboratory specimen under this specific loading history  $\sigma(x, t)$  was then derived from this sorted array. A detailed computational procedure for this part is listed in Algorithm 1.

---

**Algorithm 1** Probabilistic Time-Dependent Failure Model Algorithm

---

- 1: **for** Every material element in simulation **do**
  - 2:     Find its loading history  $\sigma(x, t)$
  - 3:     Array  $t_f\_array = []$
  - 4:     Monte Carlo sampling  $f_t, f_b, f_c \sim Prob(\sigma_N)$
  - 5:     **for** Every sampling of  $(f_t, f_b, f_c)$  **do**
  - 6:         Calculate its corresponding  $k_1, k_2, k_3$
  - 7:         Solve  $t_f$  based on Eq. 12
  - 8:         Append  $t_f$  in  $t_f\_array$
  - 9:     **end for**
  - 10:     Sort  $t_f\_array$
  - 11:     Calculate  $P_{fs}$  based on sorted  $t_f\_array$
  - 12: **end for**
- 

In order to appropriately represent strength statistics of SiC/SiC composites, a multi-scale statistical model was chosen [3, 15, 16]. Probability distribution  $Prob(\sigma_N)$  that strength parameters  $f_t$ ,  $f_b$  and  $f_c$  need to follow has the following functional form of the cumulative distribution function (CDF) in Eq. 18. It was shown that  $Prob(\sigma_N)$  can be approximated as a Gaussian distribution onto which a Weibull distribution (or equivalently a power-law function) is grafted at a probability of  $10^{-4}$  to  $10^2$ , i.e.

$$Prob(\sigma_N) = \begin{cases} 1 - e^{(\sigma_N/s_o)^m} & (\sigma_N \leq \sigma_{gr}) \\ P_{gr} + \frac{r_f}{\delta_G \sqrt{2\pi}} \int_{\sigma_{gr}}^{\sigma_N} e^{-\frac{(\sigma - \mu_G)^2}{2\delta_G^2}} d\sigma & (\sigma_N \geq \sigma_{gr}) \end{cases} \quad (18)$$

In Eq. 18,  $m$  and  $s_0$  are Weibull modulus and the scale parameter of the Weibull tail;  $\mu_G$  and  $\delta_G$  are mean and standard deviation of the Gaussian core, if considered extended to  $-\infty$ ;  $r_f$  is scaling parameter required to normalize the grafted CDF such that  $P_1(\infty) = 1$ ;  $\sigma_{gr}$  is grafting stress and  $P_{gr} = 1 - e^{-(\sigma_{gr}/s_0)^m}$  is grafting probability between  $10^{-4}$  to  $10^2$ ; The continuity of the probability density function (PDF) at the grafting point requires that  $[dP_1/dx]_{\sigma_{gr}^+} = [dP_1/dx]_{\sigma_{gr}^-}$ . Specific parameter values chosen for this statistical model would come from a set of laboratory experiments of different loading paths. However, since none multi-axial histogram tests have been conducted for SiC/SiC specimens so far, parameters such as Weibull modulus  $m$  and standard derivation  $\delta_G$  cannot be determined specifically now. In this paper, We would use published deterministic test results as the mean values  $\mu_G$  of our strength parameters [5]. They were derived from material constants  $k_1 = 5.5 \times 10^{-5} \text{ MPa}^{-2}$ ,  $k_2 = -3.7 \times 10^{-5} \text{ MPa}^{-2}$  and  $k_3 = 0.9 \times 10^{-5} \text{ MPa}^{-2}$ . We would set  $m = 20$  for uniaxial tension, bi-axial tension and uniaxial compression PLS, which is in the range of typical values for ceramic material. Standard derivation  $\delta_{ft}$ ,  $\delta_{fb}$  and  $\delta_{fc}$  were chosen to be 25 MPa, 25 MPa, and 30 MPa respectively and grafting probability  $P_{gr}$  was chosen to be  $3 \times 10^{-2}$  for all. Other parameters such as  $r_f$ ,  $s_0$  and  $\sigma_{gr}$  can be calculated based on above known parameters and distribution relations. As explained before, this multi-scale statistical model together with the finite weakest link model, fully describes the gradual change from ductile to brittle behaviour of quasi-brittle material of different sizes, which can overcome the inapplicability of the Weibull distribution for design extrapolation.

After all the failure probabilities for laboratory specimens  $P_{fs}$  under various loading history in thermo-mechanical analysis were calculated, we then used Eq. 16 to sum up all the elements' failure value and calculate the failure probability for entire cladding. Till now, we went through the whole procedure of performing reliability analysis on SiC/SiC cladding that simulated under normal operation conditions. We ran our analysis with various of kinematic constant  $n$  and cladding lengths  $L$  in order to illustrate our model can accommodate the difficulty in counting stress-time evolution and design extrapolation. We presented our results in the subsequent section.

## 5. Results and Discussion

In Figure 4, we presented the failure probability of one specimen with the uniform stress profile illustrated in Figure 2. Within first 5 months, as stress mostly stays in its compression region, failure probability tends to be zero. When tensile stress starts to generate and increases linearly with respect to time, failure probability of the specimen increases almost exponentially and stays peak at the end of 24 months. This relation can be explained by the damage kinematic we proposed in Eq. 8, as the damage growth rate can be approximated linearly proportional to  $n$ -th power of stress. Moreover, compared to time-independent model, failure probability in our model would always increase. This phenomena obeys the intrinsic idea of damage growth mechanism. Once the damage initializes and propagates, the structure would not be reversely healed and its capacity of resisting to load would continuously decrease. In Figure 5, we showed the failure probability along the height of inner surface. It can be seen that the log scale profile of failure probability also matches the stress profile showed in Figure 3. This indicates that the failure of the entire structure is most likely to be governed by high stress region. In Figure 6, the failure probability of our time-dependent model with different growth rate coefficients  $n$  were presented. With the increase value of  $n$ , the failure probability of the entire structure would decrease and approach time-independent results. This trends can also be revealed by Eq. 8. For a monotonically increasing loading history, as  $n$  approaches  $\infty$ , the damage growth is only dependent on the maximum stress state which is the current stress state. So the time-dependent model would conform to time-independent model. And since failure is only depend on current stress level but not on the combination of stress history, the failure probability would become smaller. This means our time-dependent model would outcome a higher failure probability which leads to a more conservative design. It can also shown that, with typical values of  $n$  ranging from 20 to 50, the failure

probability of the entire structure can dramatically varies from close to 1 to only 0.001. This indicates  $n$ 's value need to be carefully determined by calibration tests and its sensitivity to perturbation need to be analyzed in future. Currently calibration tests are performed by applying SiC/SiC composites with same loading configuration but different loading rate.  $n$  values can be reversely calculated based on Eq. 11 with the measurement of ultimate stress. We also showed in Figure 7 the failure probability of SiC/SiC structures with different sizes. As shown in the figure, failure probability of the entire structure would increase linearly at log scale with the increase of specimen size. From that, we demonstrated the benefit of using finite weakest link model. The failure probability of entire structure not only depends on the stress history, but is also a function of structure size. Larger structure is more vulnerable and the framework which extrapolates smaller lab test specimen results to predict large structure performance is critical.

## 6. Conclusions

**Acknowledgment:** The authors acknowledge the financial support provided by the Nuclear Engineering University Program of the Department of Energy under grant DE-NE0008785.

## References

- [1] Z. P. Bažant, J.-L. Le, and M. Z. Bazant. Scaling of strength and lifetime distributions of quasibrittle structures based on atomistic fracture mechanics. *Proc. Nat'l. Acad. Sci., USA*, 106:11484–11489, 2009.
- [2] Z. P. Bazant and J.-L. Le. *Probabilistic Mechanics of Quasibrittle Structures: Strength, Lifetime, and Size Effect*. Cambridge University Press, 2017.
- [3] Zdeněk P. Bažant and Sze-Dai Pang. Activation energy based extreme value statistics and size effect in brittle and quasibrittle fracture. *Journal of the Mechanics and Physics of Solids*, 55(1):91–131, 2007.
- [4] M. Ben-Belgacem, V. Richet, K.A. Terrani, Y. Katoh, and L.L. Snead. Thermo-mechanical analysis of lwr sic/sic composite cladding. *Journal of Nuclear Materials*, 447(1):125 – 142, 2014.
- [5] Fabien Bernachy-Barbe, Lionel Gélébart, Michel Bornert, Jérôme Crépin, and Cédric Sauder. Anisotropic damage behavior of sic/sic composite tubes: Multiaxial testing and damage characterization. *Composites Part A: Applied Science and Manufacturing*, 76:281 – 288, 2015.
- [6] C.P. Deck, G.M. Jacobsen, J. Sheeder, O. Gutierrez, J. Zhang, J. Stone, H.E. Khalifa, and C.A. Back. Characterization of sic–sic composites for accident tolerant fuel cladding. *Journal of Nuclear Materials*, 466:667 – 681, 2015.
- [7] Yangbin Deng, Koroush Shirvan, Yingwei Wu, and Guanghui Su. Probabilistic view of sic/sic composite cladding failure based on full core thermo-mechanical response. *Journal of Nuclear Materials*, 507:24–37, 2018.
- [8] A. Haldar and S. Mahadevan. *Probability, Reliability, and Statistical Methods in Engineering Design*. Wiley, New York, 2000.
- [9] L. Kachanov. *Introduction to continuum damage mechanics*. Springer Netherlands, Dordrecht, 1986.
- [10] M. Kachanov. On the concept of damage in creep and in the brittle-elastic range. *Int J Damage Mech*, 3:329–337, 10 1994.

- [11] Yutai Katoh, Kazumi Ozawa, Chunghao Shih, Takashi Nozawa, Robert J. Shnavski, Akira Hasegawa, and Lance L. Snead. Continuous sic fiber, cvf sic matrix composites for nuclear applications: Properties and irradiation effects. *Journal of Nuclear Materials*, 448(1):448 – 476, 2014.
- [12] Daejong Kim, Hyun-Geun Lee, Ji Yeon Park, and Weon-Ju Kim. Fabrication and measurement of hoop strength of sic triplex tube for nuclear fuel cladding applications. *Journal of Nuclear Materials*, 458:29 – 36, 2015.
- [13] Jacques Lamon. *Chemical Vapor Infiltrated SiC/SiC Composites (CVI SiC/SiC)*, pages 55–76. Springer US, Boston, MA, 2005.
- [14] J.-L. Le. Size effect on reliability indices and safety factors of quasibrittle structures. *Struct. Saf.*, 52:20–28, 2015.
- [15] Jia-Liang Le and Zdeněk P. Bažant. Strength distribution of dental restorative ceramics: Finite weakest link model with zero threshold. *Dental Materials*, 25(5):641–648, 2009.
- [16] Jia-Liang Le, Zdeněk P. Bažant, and Martin Z. Bazant. Unified nano-mechanics based probabilistic theory of quasibrittle and brittle structures: I. strength, static crack growth, lifetime and scaling. *Journal of the Mechanics and Physics of Solids*, 59(7):1291–1321, 2011.
- [17] Takashi Nozawa, Sunghun Kim, Kazumi Ozawa, and Hiroyasu Tanigawa. Stress envelope of silicon carbide composites at elevated temperatures. *Fusion Engineering and Design*, 89(7):1723–1727, 2014. Proceedings of the 11th International Symposium on Fusion Nuclear Technology-11 (ISFNT-11) Barcelona, Spain, 15-20 September, 2013.
- [18] Y. N. Rabotnov. *Creep Problem in Structural Members*. North-Holland, Amsterdam, 1969.
- [19] Eric Rohmer, Eric Martin, and Christophe Lorrette. Mechanical properties of sic/sic braided tubes for fuel cladding. *Journal of Nuclear Materials*, 453(1):16 – 21, 2014.
- [20] L. Saucedo-Mora, T. Lowe, S. Zhao, P.D. Lee, P.M. Mummery, and T.J. Marrow. In situ observation of mechanical damage within a sic-sic ceramic matrix composite. *Journal of Nuclear Materials*, 481:13–23, 2016.
- [21] Kirill Shapovalov, George M. Jacobsen, Luis Alva, Nathaniel Truesdale, Christian P. Deck, and Xinyu Huang. Strength of sicf-sicm composite tube under uniaxial and multiaxial loading. *Journal of Nuclear Materials*, 500:280 – 294, 2018.
- [22] Gyanender Singh, Steve Gonczy, Christian Deck, Edgar Lara-Curzio, and Yutai Katoh. Inter-laboratory round robin study on axial tensile properties of sic-sic cmc tubular test specimens. *International Journal of Applied Ceramic Technology*, 15(6):1334–1349, 2018.
- [23] Gyanender Singh, Kurt Terrani, and Yutai Katoh. Thermo-mechanical assessment of full sic/sic composite cladding for lwr applications with sensitivity analysis. *Journal of Nuclear Materials*, 499:126 – 143, 2018.
- [24] J.G. Stone, R. Schleicher, C.P. Deck, G.M. Jacobsen, H.E. Khalifa, and C.A. Back. Stress analysis and probabilistic assessment of multi-layer sic-based accident tolerant nuclear fuel cladding. *Journal of Nuclear Materials*, 466:682–697, 2015.
- [25] Kurt A. Terrani, Bruce A. Pint, Chad M. Parish, Chinthaka M. Silva, Lance L. Snead, and Yutai Katoh. Silicon carbide oxidation in steam up to 2 mpa. *Journal of the American Ceramic Society*, 97(8):2331–2352, 2014.

- [26] E. Vanmarcke. *Random Fields Analysis and Synthesis*. World Scientific Publishers, Singapore, 2010.
- [27] W. Weibull. The phenomenon of rupture in solids. *Proc. Royal Sweden Inst. Engrg. Res.*, 153:1–55, 1939.
- [28] W. Weibull. A statistical distribution function of wide applicability. *J. Appl. Mech. ASME*, 153(18):293–297, 1951.
- [29] S.J. Zinkle, K.A. Terrani, J.C. Gehin, L.J. Ott, and L.L. Snead. Accident tolerant fuels for lwrs: A perspective. *Journal of Nuclear Materials*, 448(1):374 – 379, 2014.

## List of Figures

1	Overview of our reliability analysis . . . . .	12
2	Variation of axial and hoop stress with time, at axial mid-plane of the inner surface . . . .	13
3	Variation of axial and hoop stresses with height, at the inner surface and end of 24 months	14
4	Specimen failure probability with time, stress at axial mid-plane of the inner surface . . . .	15
5	Specimen failure probability with height, at the inner surface and end of 24 months . . . .	16
6	Cladding failure probability with different n values . . . . .	17
7	Failure probability for different lengths of cladding . . . . .	18

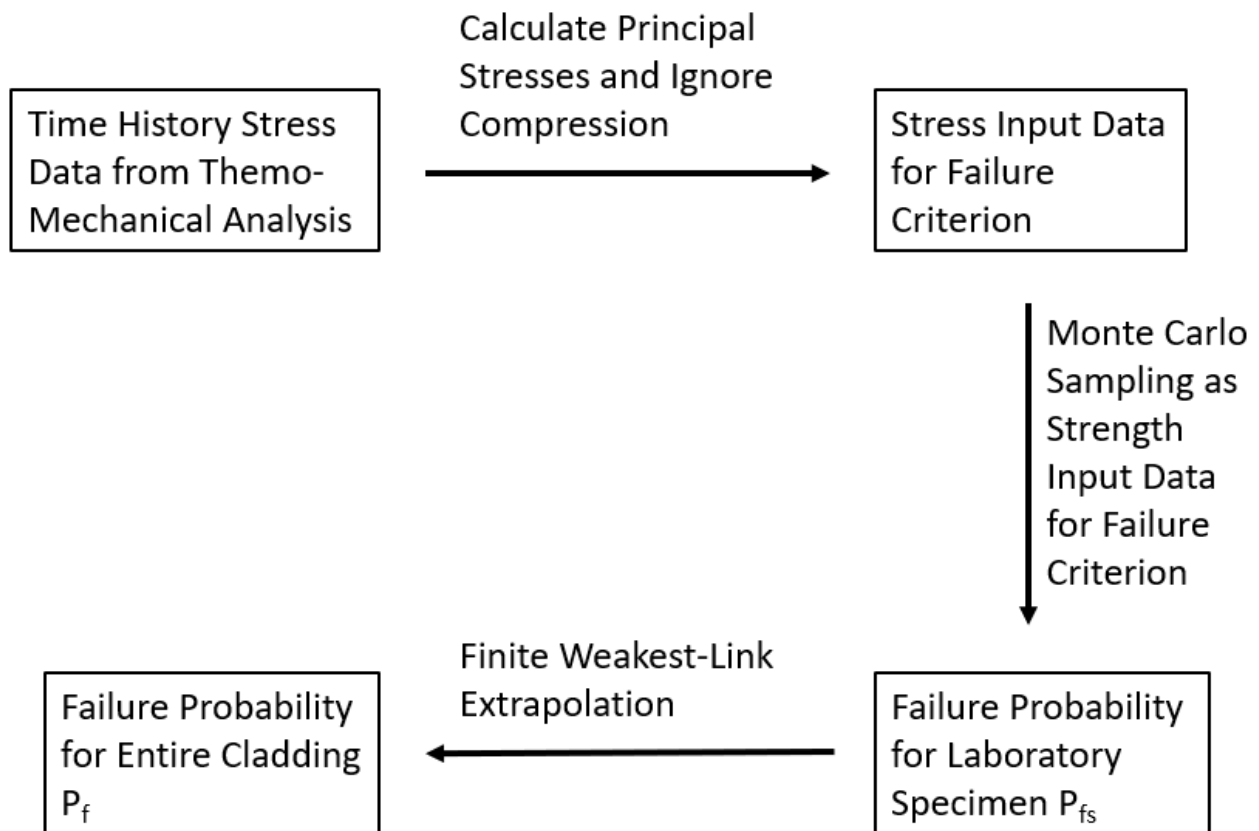


Figure 1: Overview of our reliability analysis .

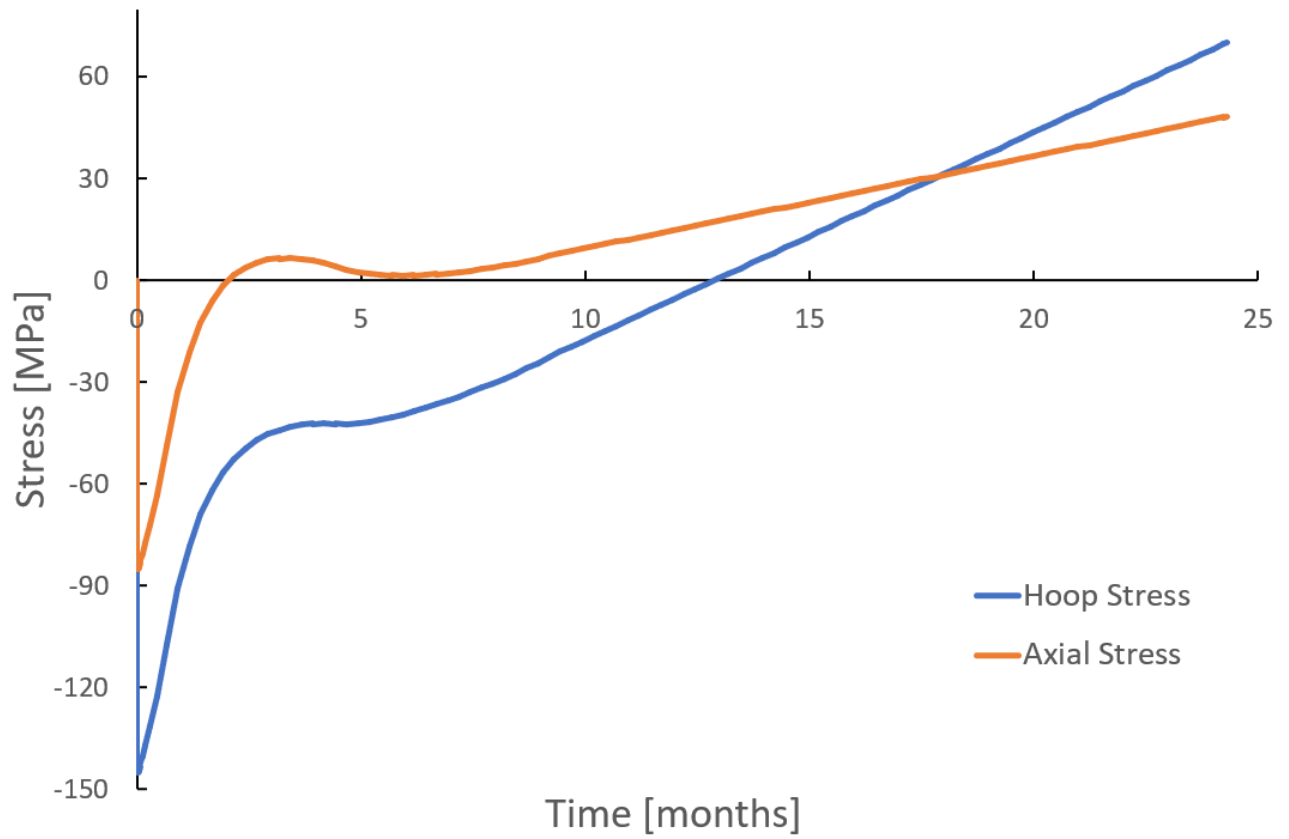


Figure 2: Variation of axial and hoop stress with time, at axial mid-plane of the inner surface .

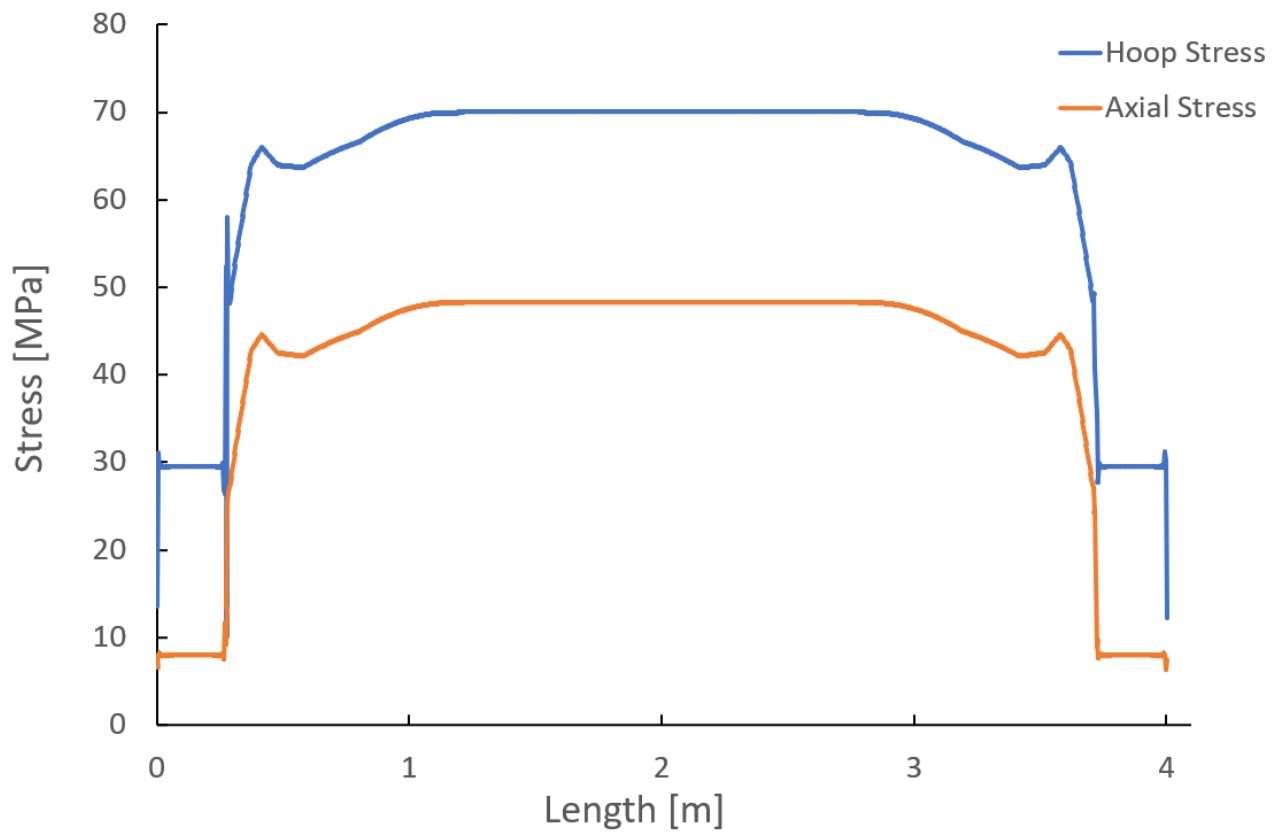


Figure 3: Variation of axial and hoop stresses with height, at the inner surface and end of 24 months

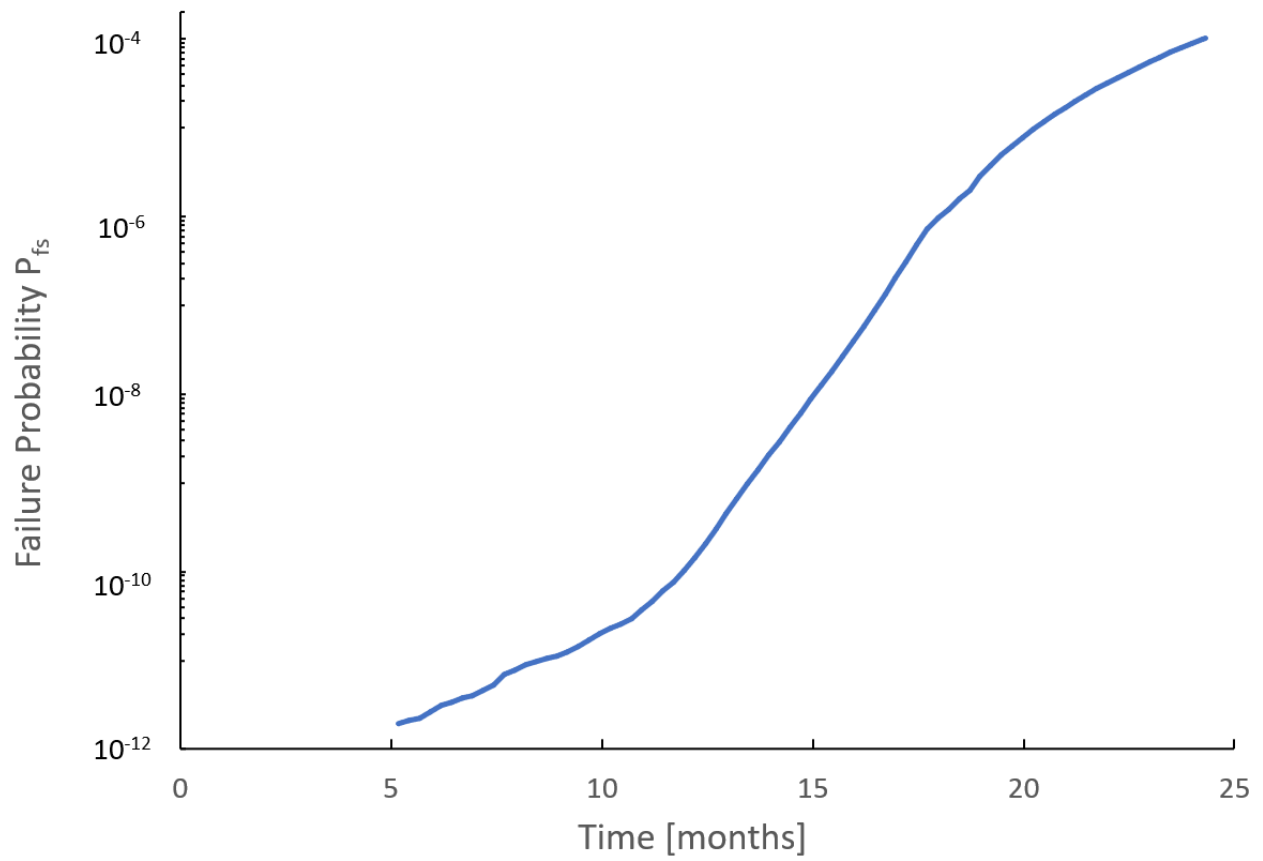


Figure 4: Specimen failure probability with time, stress at axial mid-plane of the inner surface .

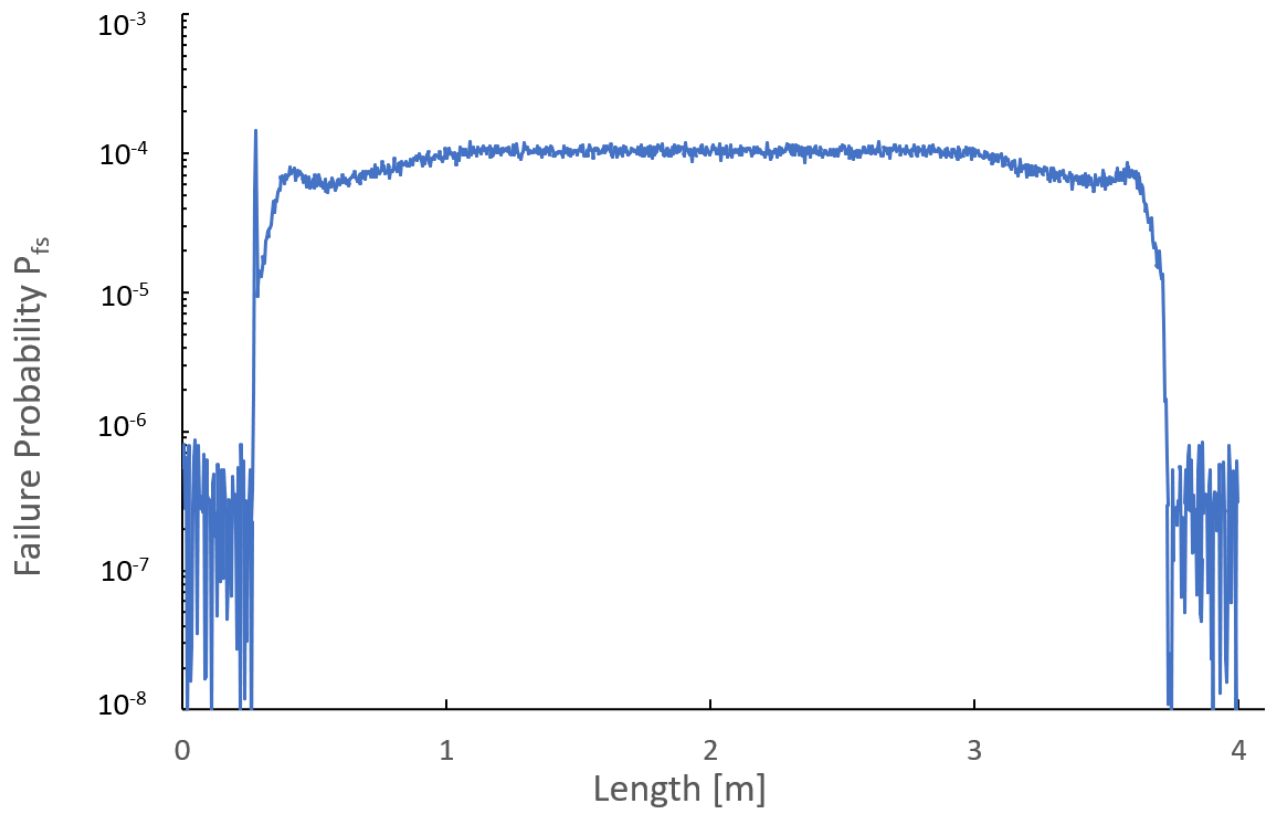


Figure 5: Specimen failure probability with height, at the inner surface and end of 24 months

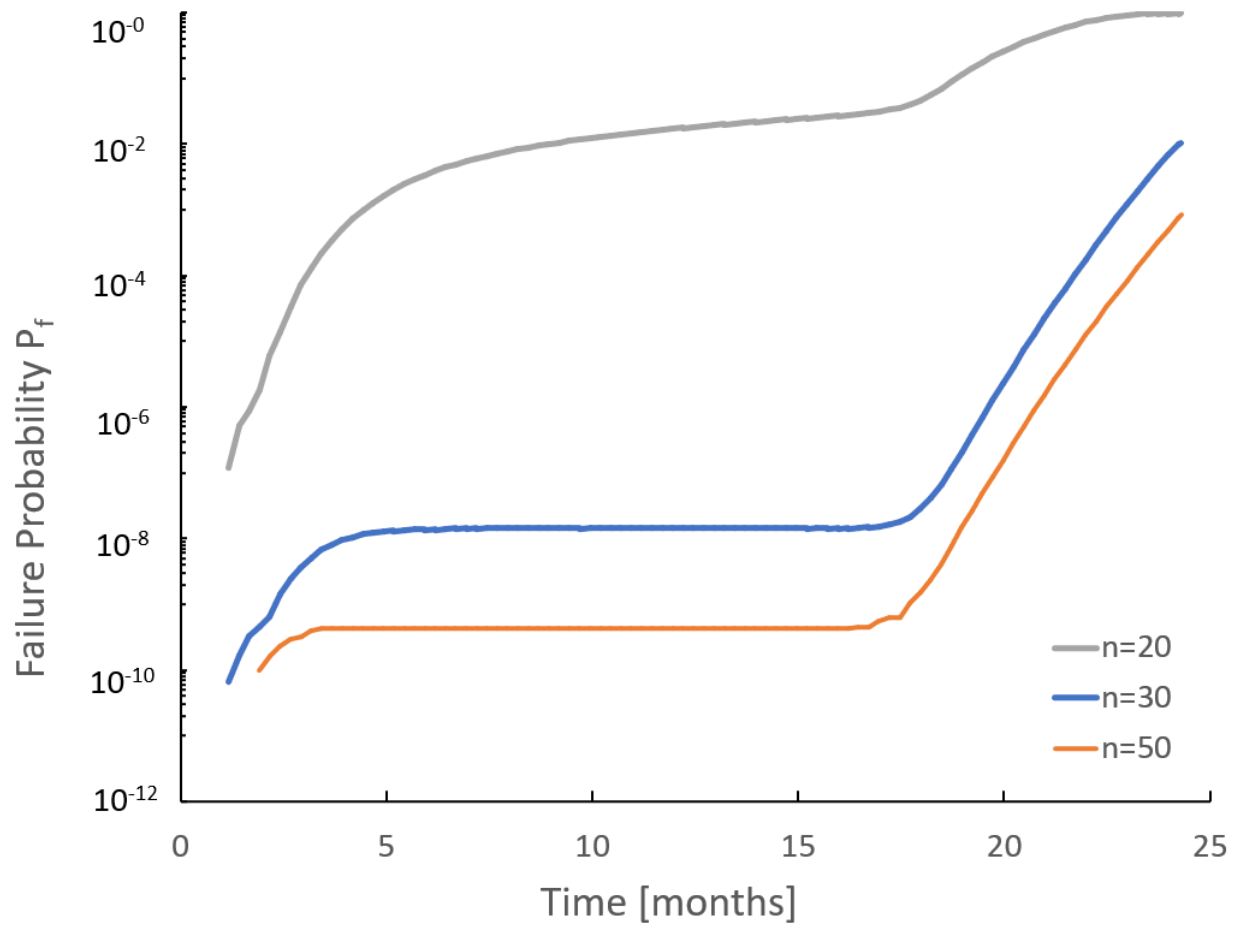


Figure 6: Cladding failure probability with different  $n$  values .

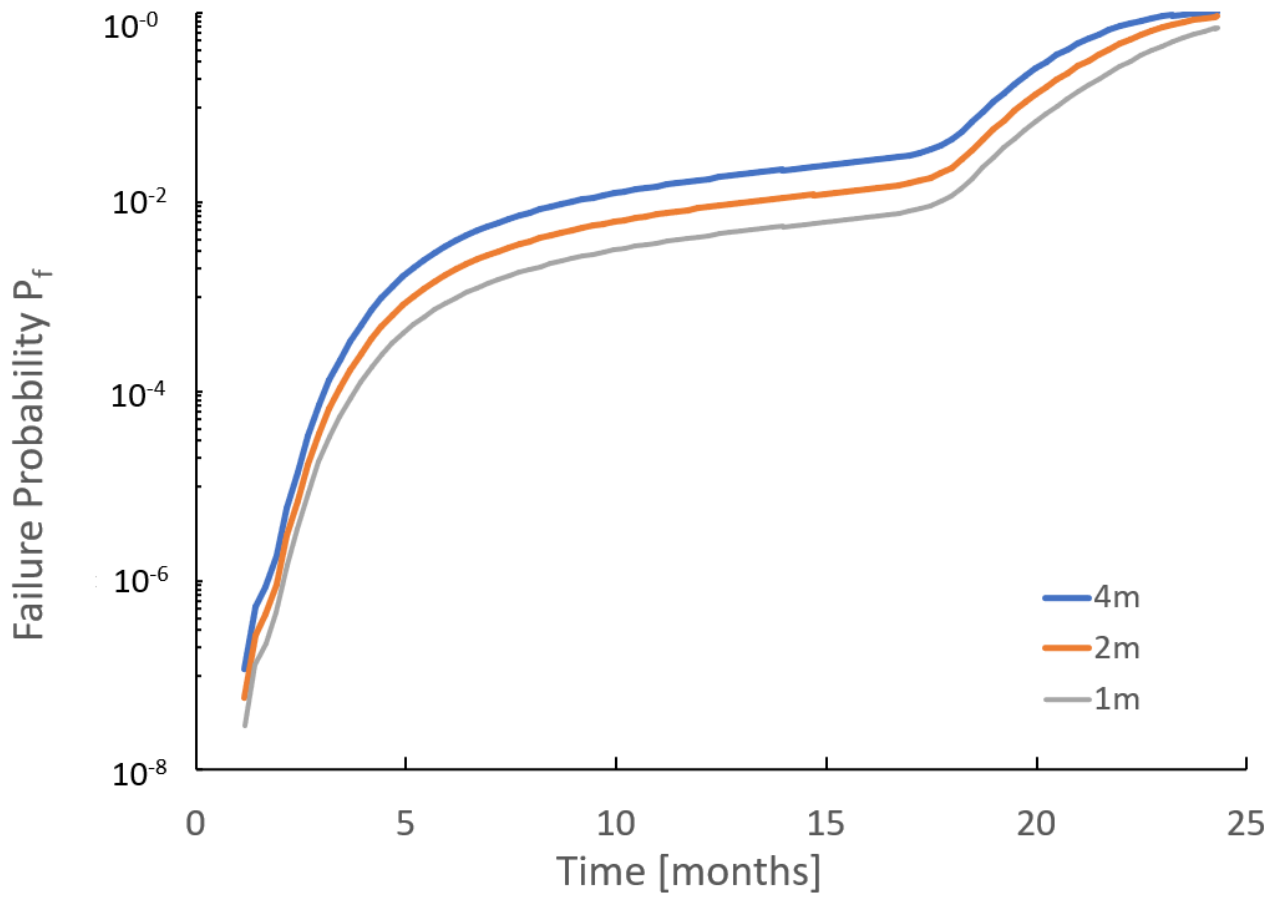


Figure 7: Failure probability for different lengths of cladding .